CRITICAL CONDITIONS FOR MELT RETENTION DURING INDUCTION MELTING IN A COLD CRUCIBLE

A. G. Merzhanov, V. A. Raduchev,
É. N. Rumanov, and A. S. Shteinberg

UDC 537.226:536.421.1

The method of induction melting in a cold crucible (CCIM), originally developed for refractory oxides [1-3], is being used more and more in the production of high-melting dielectrics. An important stage in CCIM (preceding crystallization) is the period when a steady-state thermal regime is maintained. Here, heat losses from the melt are offset by absorption of energy from the high-frequency field. The temperature of the melt and the width of the solid-phase layer are determined from the heat balance condition. The subject of the thermal stability of the phase boundary was investigated in [1], while qualitative considerations were addressed in [4]. The given system obviously has two stable states in an HF field: 1) a cold, nonabsorbent solid phase; 2) the melt, the high temperature of which is maintained by HF absorption. Along with the stable regime, there is an unstable regime with a melt of smaller radius. The union of the stable and unstable solutions yields the critical conditions for existence of the melt.

Here, we quantitatively study the stability of the melt and determine the critical conditions from the simultaneous solution of thermal and electrodynamic problems (in contrast to [5-7]). The characteristics of the steady-state regimes are obtained in relation to parameters assigned as part of the conditions of the experiment (the voltage and frequency of the HF generator, the diameter of the crucible, etc.). Stability is studied in a quasi-steady approximation.

1. Formulation of the Problem. We used the model shown in Fig. 1 to analyze the thermal stability of the melt in the HF field. The infinite conducting melt 1 is coaxial with the infinite solenoid 4 (induction coil). A layer of solid phase 2 (crust) exists between the melt and the cooled wall of the crucible 3, which is transparent with respect to the HF field. The Stefan condition below is satisfied at the phase boundary [8]

$$\rho L(da/dt) = q_+ - q_-, \tag{1.1}$$

where ρ is the density of the dielectric; L is the heat of phase transformation; a is the radius of melt; t is time; q_+ and q_- are the heat flows at the phase boundary from the direction of the melt and the solid phase, respectively.

In the steady-state regime of CCIM, the phase boundary is stationary [(da/dt) = 0]. Its position is determined from the solution of the equation $q_+(a) - q_-(a) = 0$. The values of the fluxes q_+ and q_- are calculated from the heat conduction equation.

The heat conduction equation, describing the thermal state of the dielectric in the steady-state regime, has the following form in a cylindrical coordinate system

$$\frac{\lambda}{r}\frac{d}{dr}\left(r\frac{dT}{dr}\right) + Q(r) = 0. \tag{1.2}$$

Here, r is the running radius; T is the temperature; λ is the thermal conductivity; Q is a function of the source of the heat release.

The boundary conditions for Eq. (1.2):

$$r = 0,\ dT/dr = 0;\ r = b,\ T = T_0 \tag{1.3}$$

[b is the radius of the crucible and T_0 is the temperature of the crucible (the latter is kept constant)].

2. Heating Capacity in the Dielectric. To calculate the source function Q(r), we will use the model of an infinite conducting cylinder which is positioned coaxially with the

Chernogolovka. Translated from Zhurnal Prikladnoi Mekhaniki i Tekhnicheskoi Fiziki, No. 1, pp. 78-84, January-February, 1990. Original article submitted March 25, 1987; revision submitted August 9, 1988.

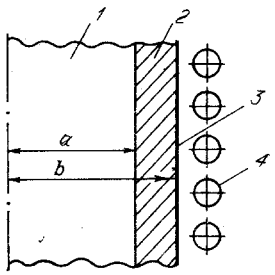

Fig. 1

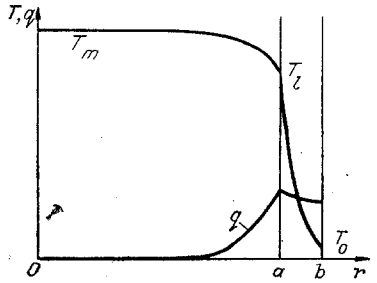

Fig. 2

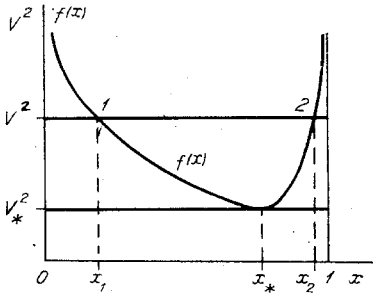

Fig. 3

infinite solenoid shown in Fig. 1. The electrical conductivity of the crust is assumed to be zero, so that no heat is released in the solid phase of the dielectic.

The heating capacity per unit volume of the melt

$$Q(r) = (\sigma/2)|j(r)|^2, \tag{2.1}$$

where σ is the electrical conductivity of the melt; j is the current density in the melt. It depends on the distribution of the magnetic field H(r) in the dielectric

$$j(r) = -(c/4\pi)[\partial H(r)/\partial r] \tag{2.2}$$

(c is the speed of light). The distribution of the field H(r) is known (see [9]):

$$H(r) = \begin{cases} H_0[J_0(\sqrt{2i}r/\delta)/J_0(\sqrt{2i}a/\delta)], & 0<r<a, \\ H_0, & a<r<b. \end{cases} \tag{2.3}$$

Here, H_0 is the strength of the magnetic field in the crust; δ is the depth of penetration of the melt by the field (the width of the skin layer); J_0 is a zeroth-order Bessel function of the first kind. Insertion of (2.2) and (2.3) into (2.1) gives us the relationship between the heat flux generated in the melt Q(r) and the strength of the magnetic field H_0:

$$Q(r) = \sigma^{-1}(c/4\pi\delta)^2|H_0|^2|g(a/\delta)|^2\varphi(r). \tag{2.4}$$

The dimensionless functions g(a/δ) and φ(r) are determined by the expressions

$$g(a/\delta) = J_1(\sqrt{2i}a/\delta)/J_0(\sqrt{2i}a/\delta),$$

$$\varphi(r) = \begin{cases} |J_1(\sqrt{2i}r/\delta)/J_1(\sqrt{2i}a/\delta)|^2, & 0<r<a, \\ 0, & a<r<b, \end{cases}$$

where J_1 is a first-order Bessel function of the first kind. In the case $\delta/a \ll 1$, the Bessel function ratio can be approximated by the exponential relation

$$\varphi(r) \approx \begin{cases} \exp[2(r-a)/\delta], & 0<r<a, \\ 0, & a<r<b. \end{cases}$$

It follows from Eq. (2.4) that calculation of the heat source Q(r) reduces to calculation of the strength of the magnetic field H_0 as a function of the parameters of the HF unit for CCIM (working frequency, number of turns of the induction coil, voltages on the coil, etc.).

The electromotive force in one turn of the solenoid in Fig. 1

$$\mathscr{E}_1 = Z(\omega)I, \tag{2.5}$$

(Z is the impedance of the turn; I is the current in the solenoid; ω is the angular frequency). In accordance with [9],

$$Z = -(i\omega/c^2)L_e + (1+i)(b/\sigma_i a_i \delta_i)[g(a_i/\delta_i)]^{-1}. \tag{2.6}$$

Here, L_e is the external part of the self-inductance of the solenoid turn; b is the radius of the solenoid (for simplicity, we assume that the latter coincides with the radius of the crucible); σ_i is the electrical conductivity of the solenoid; δ_i is the width of the skin layer in the solenoid; a_i is the radius of the conductor used to make the solenoid.

Insertion of (2.6) into (2.5) with allowance for the fact that the magnetic flux through the area of the solenoid turn

$$\Phi = (L_e/c)\,I = 2\pi \int_0^b H(r)\,r dr,$$

gives us the equation

$$\mathscr{E}_1 = -2i\pi\,(\omega/c) \int_0^b H(r)\,r dr + (1+i)(bI/\sigma_i a_i \delta_i)\,[g\,(a_i/\delta_i)]^{-1}. \tag{2.7}$$

Having used (2.3) to calculate the integral $\int_0^b H(r)\,r dr$ and having expressed the current in the solenoid I through the strength of the field H_0 (see [9]) $I = (ch/4\pi N)H_0$, we can reduce (2.7) to the form

$$\mathscr{E}_1 = -i\pi\,(\omega/c)\,H_0 \left\{ b^2 - a^2 + (1-i)\left[a\delta g\,(a/\delta) - \frac{bh\delta_i}{2\pi N a_i g\,(a_i/\delta_i)} \right] \right\}, \tag{2.8}$$

where h is the height of the solenoid and N is the number of turns in it.

The electromotive force in a solenoid with N turns has the form $\mathscr{E} = N\mathscr{E}_1$. Taking this relation into account, we easily obtain the desired expression from (2.8)

$$H_0 = (ic/\pi\omega N)\,\mathscr{E} \left\{ b^2 - a^2 + (1-i)\left[a\delta g(a/\delta) - \frac{bh\delta_i}{2\pi N a_i g\,(a_i/\delta_i)} \right] \right\}^{-1}.$$

Insertion of H_0 into (2.4) makes it possible to describe the source function as

$$Q(r) = Q_0 \varphi(r), \tag{2.9}$$

where

$$Q_0 = (\sigma/2)(U\delta/\pi N b^2)^2 |g(a/\delta)|^2 |1 - (a/b)^2 + (1-i)\{(a\delta/b^2)g(a/\delta) - [h\delta_i/2\pi N b a_i g(a_i/\delta_i)]\}|^{-2} \tag{2.10}$$

($U = |\mathscr{E}|/\sqrt{2}$ is the voltage on the solenoid).

3. Solution of the Heat Conduction Equation. The thermal conductivity of the dielectric λ is a function of temperature: it is considerably higher for the melt than for the crust. Approximation of λ by a piecewise-linear function

$$\lambda = \begin{cases} \lambda_a, & 0 < r < a, \\ \lambda, & a < r < b \end{cases} \tag{3.1}$$

makes it possible to reduce nonlinear problem (1.2)-(1.3) to the solution of two linear equations of heat conduction – in the melt (0 < r < a) and in the slag crust (a < r < b). To combine the solutions, we used the condition at the phase boundary

$$r = a, \quad T = T_l, \tag{3.2}$$

where T_l is the melting point of the dielectric. The value of a is found from the heat balance condition $q_+ = q_-$.

If we integrate Eqs. (1.2) with the source (2.9) together with boundary conditions (1.3), (3.2) while allowing for Eq. (3.1), we can find the temperature distribution T(r) and heat flux q(r) in the dielectric:

in the solid phase a < r < b

$$T = T_l - (T_l - T_0)\ln(r/a)\,[\ln(b/a)]^{-1}, \quad q = (\lambda/r)(T_l - T_0)\,[\ln(b/a)]^{-1}; \tag{3.3}$$

in the melt 0 < r < a

$$T = T_l + (Q_0/\lambda_a) \int_r^a r^{-1} \left[\int_0^r \varphi\,(r)\,r dr \right] dr, \quad q = (Q_0/r) \int_0^r \varphi\,(r)\,r dr. \tag{3.4}$$

The maximum temperature at the center of the melt

$$T_m = T_l + (Q_0/\lambda_a) \int_0^a r^{-1} \left[\int_0^r \varphi\,(r)\,r dr \right] dr.$$

The condition $\delta/a \ll 1$ is usually satisfied in CCIM processes. Thus

$$T_m \approx T_l + (Q_0 \delta^2/4\lambda_a).$$

The distribution of temperature T(r) and heat flux q(r) in the dielectric is shown in Fig. 2.

4. Heat Balance at the Phase Boundary. At r = a, Eqs. (3.3) and (3.4) determine the heat fluxes to the phase boundary from the direction of the melt q_+ and the direction of the crust q_-. The steady-state melting regime is characterized by the equality of these fluxes

$$Q_0 \int_0^a \varphi(r)\, r dr = \lambda (T_l - T_0) [\ln (b/a)]^{-1}. \tag{4.1}$$

In accordance with (2.10), the heating capacity Q_0 depends on the position on the phase boundary a. Insertion of (2.10) into (4.1) yields an equation which determines the position of the phase boundray in the steady-state thermal regime:

$$(\sigma/2)(U\delta/\pi N b^2)^2 |g(a/\delta)|^2 |1 - (a/b)^2 + (1-i)\{(a\delta/b^2) g(a/\delta) -$$
$$[h\delta_i/2\pi N b a_i g(a_i/\delta_i)]\}|^{-2} \int_0^a \varphi(r)\, r dr = \lambda (T_l - T_0) [\ln (b/a)]^{-1}.$$

It is more convenient to analyze this expression in dimensionless form

$$V^2 = 2(\pi/\alpha)^2 \left[\ln (1/x) \int_0^x \varphi(\xi)\, \xi d\xi\right]^{-1} |g(x/\alpha)|^{-2} |1 - x^2 + \alpha(1-i)\{x g(x/\alpha) - [\gamma/2\pi\beta g(\beta/\alpha)]\}|^2. \tag{4.2}$$

Here, x = a/b is the dimensionless coordinate of the phase boundary (the radius of the melt); $\alpha = \delta/b$ is the dimensionless depth of penetration of the HF field into the melt; $\xi = r/b$ is the variable of integration; $V = \sigma^{1/2}(U/N)[\lambda(T_l - T_0)]^{-1/2}$ is the dimensionless voltage on the coil; $\beta = (a_i/b)(\sigma_i/\sigma)^{1/2}$, $\gamma = (h/bN)$ are parameters. The quantity α^{-2} can be interpreted as the dimensionless frequency (since it can be represented in the form $\alpha^{-2} = \omega(2\pi\sigma)(b/c)^2$), while V^2 can be regarded as the dimensionless heating capacity in the melt. Equation (4.2) makes it possible to calculate the steady-state position of the phase boundary as a function of four parameters $x = x(\alpha, \beta, \gamma, V)$.

5. Steady-State CCIM Regimes. Figure 3 shows the qualitative behavior of the right side of Eq. (4.2), designated as f(x). The solutions of Eq. (4.2) are the abscissas of the points of intersection of the curve f(x) with the line V^2. It is evident from the figure that certain values of the parameter $V > V^*$ correspond to the two steady states 1 and 2 (the stationary positions of the phase boundary x_1 and x_2). At a certain critical value $V = V_*$, the steady-state solutions merge ($x_1 = x_2 = x_*$), while at $V < V_*$ there is a discontinuity – steady-state equation (4.2) has no solution.

Study of the stability of steady states requires the solution of an unsteady heat conduction equation. Along with (1.1), on the phase boundary we impose the condition $r = a + \varepsilon \exp(\Omega t)$, $T_s + \tau \exp(\Omega t) = T_l$, where T_S is the steady-state temperature; ε and τ are the amplitudes of the perturbations of the steady-state radius of the melt and the stationary profile of temperature in the dielectric; Ω is a decrement determining the development of the perturbations over time.

At $|\Omega| \ll \varkappa/b^2$ (where $\varkappa$ is the diffusivity), we can restrict ourselves to a quasisteady approximation and calculate the fluxes q_+, q_- in (1.1) from the steady-state equation (1.2). It is known from the theory of the branching of dynamic systems [10] that $|\Omega| = 0$ at the point of confluence of two steady-state solutions. It follows from this that the quasisteady approximation is valid near the stability boundary (at $x \approx x_*$, when $|\Omega| \to 0$). Here, the problem is reduced to the analysis of a single equation (1.1), from which it follows that a stable steady state will exist under the condition

$$dq_+/da < dq_-/da. \tag{5.1}$$

The opposite inequality corresponds to the unstable state. Relation (5.1) is valid for a positive value of the derivative df/dx (the opposite relation is valid for a negative value). It is evident from Fig. 3 that $df/dx < 0$ for $x_1 \approx x_*$ and $df/dx > 0$ for $x_2 \approx x_*$. Thus, the steady states to the left of the critical point ($x < x_*$) are unstable; accordingly, $x_* < x < 1$ is the region of stable steady states.

In the study of stability, the quasisteady approximation rests (as noted above) on the smallness of $[\Omega]$ near the stability boundary. For a similar reason, the study of the

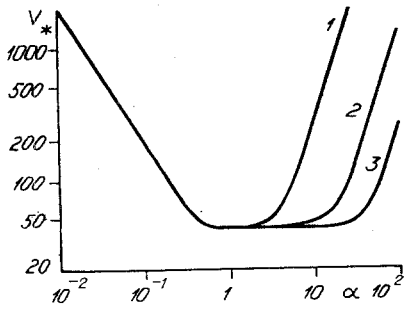

Fig. 4

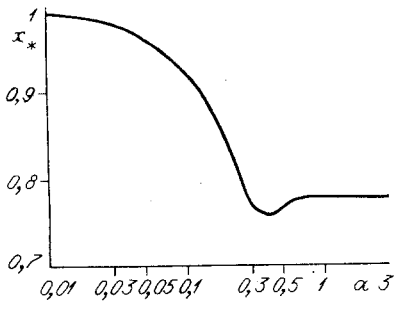

Fig. 5

stability of steady-state solutions in the theory of thermal explosions can be restricted to consideration of the regular regime [11].

The quantity x_1 can be regarded as the critical radius of the starting melt; if $x < x_1$ at the beginning of melting, then melting of the dielectric will not occur at the voltage on the coil V – the starting melt will be frozen; at $x > x_1$, a fusion wave propagates in the dielectric and, after the elapse of a certain period of time, the melt–solid system enters the stable steady state 2. This state corresponds to the melt radius x_2.

A reduction in the voltage on the coil is accompanied by descent of the line V^2 in Fig. 2 and an increase in the width of the solid phase [a smooth increase in the quantity $(1 - x_2)$ with a decrease in V signifies directional crystallization of the melt in the radial direction]. The critical voltage $V = V_*$ corresponds to the minimum melt radius x_*. A further decrease in the voltage on the coil results in spontaneous crystallization of the melt.

Figures 4 and 5 show dependences of the critical values of V_* and x_* on the parameter α calculated from Eq. (4.2). Curves 1-3 in Fig. 4 are for the following values of the parameters β and γ: 1) $\beta = 1$, $\gamma = 0.2$; 2) $\beta = 10$, $\gamma = 1$; 3) $\beta = 10$, $\gamma = 0.2$ (values typical of the CCIM of oxides); the value of x_* is independent of β and γ. It can be seen from the figures that the relations $V_*(\alpha)$ and $x_*(\alpha)$ are nonmonotonic. The appearance of the extrema can be explained as follows. The total heating capacity is the product of the volume in which heat is released and the mean heat flux. With a decrease in frequency (an increase in α), the first of these factors increases together with δ, while the second decreases – since there is a decrease in the density of the eddy currents induced in the melt by the magnetic field of the coil. At $\alpha \gtrsim 1$ $(\delta \gtrsim b)$, heat is liberated almost uniformly throughout the melt; the curve $x_*(\alpha)$ is saturated – the critical radius of the melt is independent of frequency.

In the region $\alpha \lesssim 1$, we have the relation

$$|\gamma/2\pi\beta g(\beta/\alpha)| \ll |x_* g(x_*/\alpha)|, \qquad (5.2)$$

which is connected with the smallness (in the high-frequency region) of the active resistance of the coil compared to its inductive resistance. It follows from (4.2) and (5.2) that at $\alpha \lesssim 1$ the critical value V_* is a function only of the one parameter α. In the low-frequency region (at $\alpha \gg 1$), relation (2.5) is not satisfied; it is necessary to consider the effect of the active resistance of the coil and calculate the critical value V_* as $V_* = V_*(\alpha, \beta, \gamma)$. It is evident from Fig. 4 that at $\alpha \gg 1$, V_* increases with a decrease in β and an increase in γ.

In the case of CCIM of oxides, the values $\alpha \sim 0.05$-0.1 are realized at frequencies of 1-5 MHz. At N = 1, b = 0.1 m, $\lambda = 4$ W/(m·K), $T_\ell - T_0 = 2500$ K, the minimum voltage on the coil in the indicated range of α is $U_* \sim 1$ kV. It is evident from Fig. 5 that at $\alpha = 0.05$-0.1, the relation $(1 - x_*) \ll 1$ is valid. This means that at $V < V_*$ the melt becomes thermally unstable with a thin layer of crust. In other words, it is not possible to crystallize the dielectric in the radial direction by smoothly reducing the heat liberation in the melt (such as by smoothly reducing the voltage on the coil) in the parameter region $\alpha \lesssim 0.1$. Maximum thermal stability of the melt is achieved at $\alpha = 0.3$-0.5 [the extremum of the curve $x_*(\alpha)$ in Fig. 5]. Up to 40% of the volume of the melt can be crystallized by directional crystallization in this range of α.

It should be noted that the calculated values of V_* and x_* are estimates of the lower bound, since the infinite-melt model shown in Fig. 1 does not account for boundary effects [heat loss from the melt zone in the axial direction (which occurs in actual CCIM process), nonuniformity of the magnetic field at the ends of the coil, etc.].

A charge in the form of powder with a fineness of about 10 μm is usually used as the charge in CCIM processes. The melting of the powder differs significantly from the melting of a monolithic (nonporous) dielectric. The author of [12] explained features of CCIM at the stage of fusion-wave propagation that are connected with capillary spreading of the melt in the pores of the solid phase of the dielectric: the melt impregnates the solid phase and crystallizes in it; the crystallizing layer then undergoes slow through melting. This pattern is subsequently repeated. The capillary spreading phenomen also has an effect on the steady-state CCIM regime. In this case, the following situation is possible. After the phase boundary occupies the position x_2 (the stable steady state 2 in Fig. 3), the melt impregnates the solid phase and crystallizes. The thermal conductivity of the crust suddenly increases, since the thermal conductivity of the crystallized layer is considerably greater than that of the powder charge. The jump in conductivity corresponds to a sharp reduction in V. In the case $V > V_*$, the phase boundary occupies the new steady position $x_* < x < x_2$; at $V < V_*$, a crystallization wave propagates through the dielectric from the periphery to the center.

We thank A. P. Aldushina, V. V. Grachev, I. A. Kanaev, and V. A. Knyazik for their fruitful discussion of the present study.

LITERATURE CITED

1. V. I. Aleksandrov, V. V. Osiko, A. M. Prokhorov, and V. M. Tatarintsev, "New method of producing refractory single crystals in fused ceramics," Vestn. Akad. Nauk SSSR, No. 12 (1973).
2. V. I. Aleksandrov, V. V. Osiko, A. M. Prokhorov, and V. M. Tatarintsev, "Production of high-temperature materials by direct high-frequency melting in a cold container," Usp. Khim., 47, No. 3 (1978).
3. V. I. Aleksandrov, N. A. Iofis, V. V. Osiko, et al., "Fianites and prospects for their practical use," Vestn. Akad. Nauk SSSR, No. 6 (1980).
4. A. G. Merzhanov, V. A. Raduchev, and É. N. Rumanov, "Thermal fusion waves and the crystallization of a dielectric," Dokl. Akad. Nauk SSSR, 253, No. 2 (1980).
5. Yu. B. Petrov, A. V. Shkul'kov, V. V. Nezhentsev, and I. A. Kanaev, "Analysis of the electrical characteristics of induction furnaces with a cold crucible for melting oxides," Élektrotekhnika, No. 8 (1982).
6. Yu. B. Petrov, Induction Melting of Oxides [in Russian], Énergoatomizdat, Leningrad (1983).
7. Yu. N. Smirnov, A. V. Shkul'kov, and I. A. Kanaev, "Temperature of an oxide melt in the steady-state melting regime in induction furnaces with a cold crucible," Izv. Vyssh. Uchebn. Zaved., Elektromekh., No. 9 (1984).
8. H. Carslaw and I. Jaeger, Conduction of Heat in Solids, Oxford Univ. Press, New Jersey (1959).
9. L. D. Landau and E. M. Lifshitz, Continuum Electrodynamics [Russian translation], Nauka, Moscow (1982).
10. N. N. Bautin and E. A. Leontovich, Methods and Techniques for Qualitative Study of Dynamic Systems in a Plane [in Russian], Nauka, Moscow (1976).
11. A. G. Istratov and V. B. Librovich, "Stability of solutions in the steady-state theory of thermal explosion," Prikl. Mat. Mekh., 27, No. 2 (1963).
12. É. N. Rumanov, "Fusion wave in a porous substance," Preprint, OIKhF Akad. Nauk SSSR, Chernogolovka (1982).